THE EXPERIMENTAL PROGRAM AT NAL

J. Jackson

▶ **To cite this version:**

J. Jackson. THE EXPERIMENTAL PROGRAM AT NAL. Journal de Physique Colloques, 1973, 34 (C1), pp.C1-429-C1-444. 10.1051/jphyscol:1973161 . jpa-00215241

HAL Id: jpa-00215241
https://hal.science/jpa-00215241v1

Submitted on 4 Feb 2008

HAL is a multi-disciplinary open access archive for the deposit and dissemination of scientific research documents, whether they are published or not. The documents may come from teaching and research institutions in France or abroad, or from public or private research centers.

L'archive ouverte pluridisciplinaire **HAL**, est destinée au dépôt et à la diffusion de documents scientifiques de niveau recherche, publiés ou non, émanant des établissements d'enseignement et de recherche français ou étrangers, des laboratoires publics ou privés.

THE EXPERIMENTAL PROGRAM AT NAL

J.D. JACKSON
NAL / Berkeley

1.- INTRODUCTION. - This is a progress report on the physics research program at the National Accelerator Laboratory, Batavia, Illinois as of the summer of 1973. More precisely it is the status as of July 1, 1973, before the last meeting of the NAL Program Advisory Committee. Actions on proposals subsequent to that meeting are, with few exceptions, not mentioned in this report. This causes no qualitative and very little quantitative distortion of the picture of the overall program.

The National Accelerator Laboratory was authorized and first funded in 1965. The accelerator, nominally a 200 GeV proton synchrotron with capability of ultimate operation up to 500 GeV, began functioning in 1972. The machine progress to date is indicated in Table 1 and also in figures 1 and 2.

TABLE 1

Performance Table

	July '71	Jan. '72	July '72	Jan. '73	July '73
Energy (GeV)	0	20	200	300 (400)	300
Intensity (protons/ pulse)	0	~10^9	7x10^{10}	~10^{12}	2.5x10^{12}
Expt'l Areas Operating	0	0 (1)	2	2 (3)(4)	3
Experiments in Progress at a time	0	0 (2)	4	~6	~8
Number of Completed Experiments	0	0	0	10	17

The table shows several dimensions - energy, intensity, number of experimental areas, experiments simultaneously in progress and number of completed experiments.

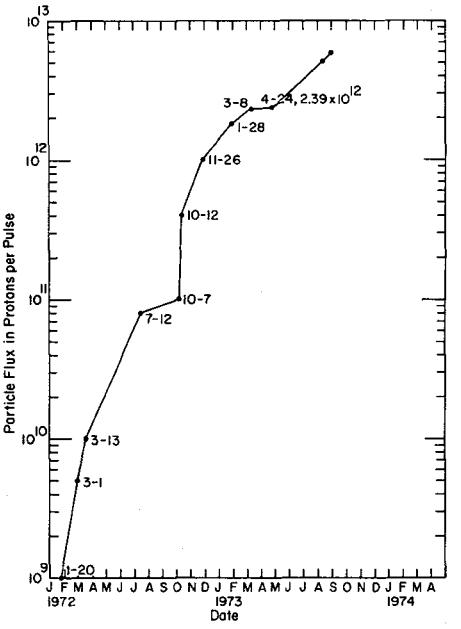

FIG. 1. - Best intensity of the circulating beam in protons per acceleration cycle as a function of calendar time up to September 1, 1973.

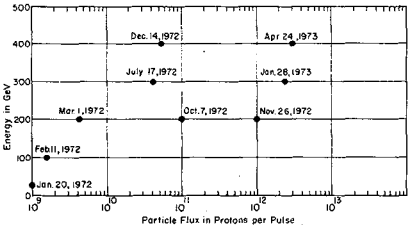

FIG. 2 . - Intensity-energy diagram with dates at which the various energies and intensities were first attained.

Article published online by EDP Sciences and available at http://dx.doi.org/10.1051/jphyscol:1973161

The machine has operated for physics at 400 GeV during 1973 and will again before the year is out. The intensity has risen in late August to 6 x 10^{12} protons per pulse at 300 GeV. The number of completed experimental runs now stands at over 20. Figures 1 and 2 indicate the progress in intensity and/or energy with time.

At the present time the "standard" operating characteristics of the machine are as follows:

Energy	300 GeV
Repetition rate	1/6 sec^{-1} at 300 GeV (1/4 sec^{-1} at 200 GeV, 1/12 sec^{-1} at 400 GeV)
Flat top	0.7 - 1.0 sec
Intensity	~(2-4) x 10^{12} protons/pulse
Extraction efficiency	90 - 95%
"Duty cycle" in extracted beam	~0.3 sec/1 sec flat top (not counting r-f structure)

Operation at 200 GeV or 400 GeV with essentially the same intensity per pulse is possible. In August, for example, both 300 GeV and 200 GeV running occurred. The extraction efficiency is adequate for the present intensities, but an appreciable increase in intensity towards the design value of 5 x 10^{13} protons/pulse must be accompanied by improved efficiency of extraction in order to avoid excess radioactivity and radiation damage. The 720 Hz ripple on the extracted beam has been reduced considerably in recent months by the use of feedback loops, but more work is necessary in order to obtain a really satisfyingly smooth spill.

Figure 3 is a schematic diagram of the accelerator complex and the various experimental areas. The longest beam line is the neutrino beam line, approximately 2 km in length, with the neutrino beam itself traversing roughly 1.3 km to the present end of the line. There are 4 experimental areas, the internal target and the meson, neutrino and proton "laboratories". The neutrino laboratory has two experimental areas, indicated by the open circles in figure 3. The meson and proton laboratories are more localized, although each has appendages that will be indicated in more detail below. The names "meson", "neutrino", "proton" do not imply any absolute restriction on the type of particles to be used as projectiles in the different laboratories, but only tendencies. The

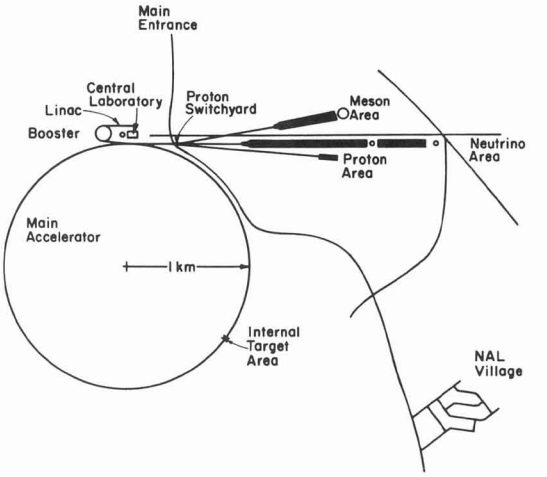

FIG. 3. - Schematic diagram of the NAL accelerator and experimental areas.

meson laboratory, for example, contains proton and neutron beams as well as several meson beams. The proton laboratory has protons incident on it, but can have arbitrary secondary beams, including photons and electrons.

The beam splitting capability is shown schematically in figure 4. The beam switchyard contains two splitters

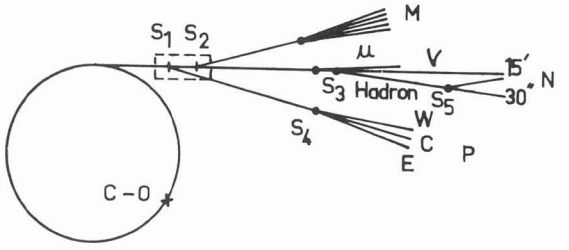

FIG. 4. - Schematic diagram of the main beam splitters for different areas. The dashed region is the main switchyard where splitters S_1 and S_2 operate to send beam to the meson lab (M) and/or the proton lab (P), and/or the neutrino lab (N).

that can deliver varying amounts of beam to all three areas. In the neutrino line splitter S_3 can send a hadronic beam to the 30" bubble chamber at the same time as neutrino and muon beams are being delivered. It is planned to install a further switch or splitter S_5 in that hadron beam in order to provide hadrons for the 15 foot and the 30 inch bubble chambers, probably on an either/or basis. Inside the meson laboratory there are further local switches or splits possible. In the proton laboratory the splitter S_4 is about to be installed and will divide beam between

the "East" and "Central" regions. At the present time delivery of beam to 2 of the 3 areas, as well as to the internal target area (obviously!), is "standard". On a good day 6 to 8 experiments get some beam.

2.- STATISTICAL ASPECTS OF THE RESEARCH PROGRAM.- The statistics on proposals and approved experiments as of July 1, 1973 are

1. Number of proposals	
Approved	80
Deferred	35
Inactive/withdrawn	47
Rejected	23
Newly proposed (some decisions since July 1)	48
Total submitted	233
2. Approved group (80)	
(a) Completed (as of Sept. 8, 1973)	
Emulsion exposures at 200 GeV	9
Bare 30" bubble chamber	6
Proton-proton elastic scattering	1
Proton-proton inelastic (inclusive)	2
Quark search	2
Photon search ($pp \rightarrow \gamma X$)	1
Total completed	21
(b) In various stages of progress	
Counter experiments	37
30" bubble chamber	6
15' bubble chamber	7
Miscellaneous (emulsions, nuclear chemistry etc.)	9
Total in progress	59

It is obvious merely from the number of approved experiments that only a sample of results and experiments in progress can be discussed. The several emulsion exposures will not be reported on (out of ignorance on my part), even though they contain some interesting results on multiparticle production from nuclei. In the following sections the approved program for each area or facility is outlined first, followed by a description of the present status of that program. Finally some representative interesting results are discussed briefly where they exist. In order to keep the physics foremost the names of the physicists and their institutions will generally be omitted, except when specific results are quoted. The interested reader can consult the official NAL lists of proposals and approved experiments for such details.

3.- BUBBLE CHAMBERS. - The bubble chambers at NAL are the 30 inch chamber formerly at Argonne National Laboratory and the new 15 foot chamber designed primarily for neutrino physics. The 30 inch chamber has been in action intermittently for somewhat more than a year, but the 15 foot chamber is just now being commissioned.

3.1.- 30 INCH "BARE" CHAMBER PROGRAM. - The aim of the early operation of the 30 inch chamber was to provide a quick survey of the main features of hadronic interactions and their energy dependences, and to see any strikingly new phenomena that might happen to exist. Proposals came in with favourite choices of energies, number of pictures, etc. but the program was arbitrarily set at a nominal 50,000 pictures per experiment at 100, 200, 300 and 400 GeV incident energies, with p, π^- and most recently π^+. The present status of the program is indicated in Table 2.

TABLE 2

30" Bubble Chamber Program

Incident Particle	Target	Energies (GeV) <100	100	200	300	400
p	H_2		32 K	70 K	50 K	12 K
π^-	H_2		50 K	48 K		
π^+	H_2		50 K			

The approximate number of pictures taken to date are shown for each experiment, with the underlining indicating completed exposures. Somewhat over 300,000 pictures have been taken. This represents considerably more than one half of the presently approved program. Typically the experiments have 5 K - 7 K events with ~ 0.2 event/μb, although some exposures have roughly double these statistics. There are a few months more of hydrogen running in the approved program. Seventeen new proposals have been received for the 30 inch chamber, covering a spectrum of physics goals with H_2, D_2 and Ne in the chamber. Out of these there will probably emerge some D_2 running at least, and perhaps some with neon.

3.2.- HYBRID OPERATION OF THE 30 INCH CHAMBER.- The above experiments are standard bubble chamber exposures for which there are serious problems with the forward cone of particles. Except for special topologies it is difficult to do more than count prongs in this forward jet. In an attempt to extend the usefulness of the 30 inch chamber a hybrid mode of operation has been developed. There is now an upstream tagging system with proportional wire chambers (necessary for the π^+ exposures in the bare chamber operation) and a downstream system of large wide gap optical spark chambers. The fringing field of the magnet of the bubble chamber provides some slight magnetic analysis and separation of the forward going particles which are then detected in the spark chambers. This hybrid system is approved for 500 K pictures and is presently running. Film from the "bare" chamber program (Table 2) is, after six months, being made available to these experimenters for those periods when they were in parasitic hybrid operation during the past year. Some preliminary results from the pictures at 200 and 300 GeV on correlations have been presented at the Berkeley and Aix-en-Provence meetings in August, 1973, but the main experiment is just nicely underway.

Anticipated to follow the optical spark chamber experiment is a more sophisticated hybrid experiment with large proportional wire chambers downstream of the bubble chamber.

3.3.- 15 FOOT BUBBLE CHAMBER.- The 15 foot bubble chamber with its superconducting magnet is nearing first operation. The magnet has been thoroughly tested and is in good shape. There have been problems, however, with the fiberglass piston. Presently a substitute steel piston is installed for the initial test runs of the chamber this fall. Eddy current heating will severely limit the magnetic field in the chamber (to less than 6 - 10 Kg, probably). The approved program is for neutrino physics, but the initial engineering run of perhaps 50 K pictures will probably be with a hadron beam. This will be useful in proving out the chamber and its optics and will also give an indication of how useful it will be for hadronic processes. The fiberglass piston is presently undergoing extensive tests at NAL, but it may be several months before installation.

There are six approved weak interaction experiments at present, neutrinos in H_2 and two different mixtures of H_2 and Ne and the corresponding exposures for anti-neutrinos. These involve large numbers of pictures, of course, and will occupy the chamber for some time. With the broad band neutrino horn presently being installed it is expected to have 1 event/10 pictures with 10^{13} protons/pulse on the target. This program will begin in early 1974. There is also the possibility of running the 15 foot chamber with D_2. This involves a sizeable amount of deuterium but seems feasible with the cooperation of other U.S. laboratories.

An external muon identifier (EMI) is under construction. In its first phase it has passive internal absorbers filling the spaces in and around the magnet coils in order to give a uniform hadronic absorption over a large solid angle and approximately 30 active external detector modules (1 m^2 each) located just outside the vacuum tank. Eventually it is hoped to cover an angular range of 60^o x 180^o in a later phase.

3.4.- A SAMPLING OF RESULTS FROM THE 30 INCH BUBBLE CHAMBER.- From Table 2 it can be seen that a number of exposures with both protons and pions have been completed. A large number of papers have been published or submitted for publication and to conferences on 100, 200, 300 and 400 GeV proton-proton experiments and early results from the 200 GeV π^-p experiment appear in the Vanderbilt Conference proceedings . The first papers in each case concern the prong cross sections, mean charged multiplicity $\langle n \rangle$; the integral correlation parameter f_2 and similar topological aspects. Later results concern inclusive distributions for pp → cX where c = π^+, π^-, K, p, Δ, Λ, γ and the differential two-particle correlations in rapidity and azimuth. Here only a small sampling of results can be mentioned.

3.4.1.- pp → pX at 200 GeV, t distributions at fixed x.- One important aspect of the inclusive proton spectrum in the large $|x|$ region ($0.75 < |x| < 1.0$) is the behaviour at very small $|t|$. In the region of $|x| \to 1$ it is expected that a triple Regge description should have approximate validity, except at the extreme kinematic limit where $M^2 \to m_N^2$. Furthermore, the triple pomeron (PPP) coupling should dominate or at least be important at NAL energies and above. Data

from the ISR at $|t| > 0.15$ (GeV/c)^2 indicate such behaviour [1]. There are theoretical arguments favouring the vanishing of the PPP vertex as $|t| \to 0$. It is of interest to see evidence of this decoupling in the behaviour of the inclusive distributions at small $|t|$ in terms of a turnover or flattening, if not a zero. Most existing counter data at the ISR and NAL are at $|t| > 0.15$ and show a smooth more or less exponential fall off in $|t|$ beyond this point. The ANL-NAL bubble chamber experiment [2] at 200 GeV has the data shown in figure 5. The statistical

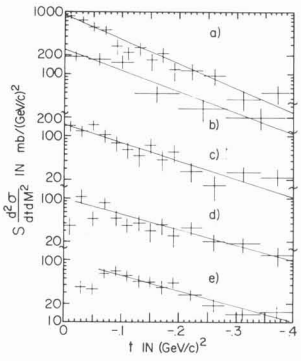

FIG. 5.- Invariant cross sections $s\, d^2\sigma/dt\, dM^2$ for $pp \to pX$ at 205 GeV ($s \simeq 387$ GeV^2) as functions of momentum transfer t for a series of intervals in M^2 (or equivalently in x). The intervals are (a) $M^2 < 5$ ($x > 0.987$), (b) $5 < M^2 < 10$ ($0.974 < x < 0.987$), (c) $10 < M^2 < 25$ ($0.935 < x < 0.974$), (d) $25 < M^2 < 50$ ($0.871 < x < 0.935$), (3) $50 < M^2 < 100$ ($0.742 < x < 0.871$). Date from reference 2.

accuracy is not high, but in the small $|t|$ region where there are 3 to 5 bins below 0.10 (GeV/c)^2 there is no evidence for a dip as $t \to 0$. The turnover seen in the M^2 intervals (d) and (e) of figure 5 is merely a $t_{min} = m^2(M^2/s)^2$ effect, the kinematic limits being $t_{min} \simeq 0.008$ and 0.033, respectively. The PPP coupling is expected to be important for $x > 0.90$ (intervals (b) and (c) of figure 5). The absence of any dip can be attributed to the presence of other triple Regge couplings at 200 GeV, but these results should bother theorists at least a little bit.

3.4.2- $pp \to p+$ (n charged prongs) $\langle n\rangle_{M^2}$ $(f_2)_{M^2}$.- By selecting the slow proton in the lab. to fix the missing mass M^2, topological cross sections can be measured as a function of M^2. One thus can measure $\langle n\rangle$, f_2, etc. for what amounts to Reggeon (Pomeron)-proton collisions with c.m.s. energy $\sqrt{s} = M$. This interpretation is indicated schematically in the inset diagram of figure 6. It is of interest to know whether the properties of pomeron-proton collisions are similar to or different from proton-proton collisions at the same c.m.s. energy. The results shown

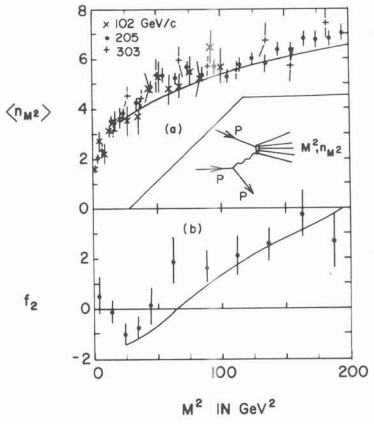

FIG. 6.- Mean charge multiplicity $\langle n\rangle_{M^2}$ and correlation parameter $(f_2)_{M^2}$ as a function of M^2 for pp interactions. (a) $\langle n\rangle_{M^2}$ for 100, 200 and 300 GeV, (b) $(f_2)_{M^2}$ for the 200 GeV data. The curves are those for proton-proton interactions at $s = M^2$. Figure from reference 2.

in figure 6 indicate a remarkable similarity for $\langle n\rangle$ and f_2 for $0 < M^2 < 200$ GeV^2. This type of data, difficult to obtain with counter experiments, has implications for our ideas on the diffractive component in multiparticle production processes.

3.4.3.- s-dependence of $\langle n\rangle$, f_2^-, inclusive spectra.- With bubble chamber data from the 30" chamber at several energies up to 400 GeV and Mirabelle data at lower energies a fairly complete picture of the energy dependences of various features of p-p interactions is available up to $s = 750$ GeV^2 and up to $s \simeq 390$ GeV^2 for $\pi^- p$ interactions. A recent fitting of $\langle n\rangle$, f_2^- and f_3^- for p-p collisions from 50 to 400 GeV by Ferbel [3] gives

$\langle n\rangle = (1.8 \pm 0.1)\ \ln s - (2.9 \pm 0.3)$

$f_2^- = (9.0 \pm 3.7) - (4.0 \pm 1.4)\ \ln s + (0.4 \pm 0.1)(\ln s)^2$

$f_3^- = (1.6 \pm 1.0) - (0.4 \pm 0.2)\ \ln s$

The mean charge multiplicity is consistent with a linear rise with $\ln s$, while f_2^- shows definite curvature when plotted versus $\ln s$. The above fits are not unique, of course. Other functional forms are possible. The preliminary value of f_2^- at 400 GeV is $f_2^- = 2.2 \pm 0.2$.

Similarly, the scaling properties of various inclusive spectra can be explored from the old energies below 25 GeV to 400 GeV. For $pp \to \pi X$ there is scaling in the fragmentation region, but a rise in the central region up to 400 GeV, a trend that continues over the ISR range. For the inclusive proton spectrum ($pp \to pX$) very near $x = 1$ the bubble chamber results at 100 and 400 GeV from the Michigan-Rochester collaboration [3] indicate a lack of scaling. Specifically, for $0.6 < |x| < 0.94$ the inclusive invariant cross section shows scaling behaviour in x at fixed $p_\perp$ within the statistical errors of 10 - 15%. But for $|x| > 0.94$ there is significant energy dependence, the cross section peaking at a higher value at $x = 1$ and falling off more rapidly away from $x = 1$ at 400 GeV than at 100 GeV. This behaviour is consistent with other indications from NAL (see below) and with theoretical ideas that non-scaling contributions (e.g. in triple Regge language, PPR or PRR' terms) can be most important at $x \simeq 1^-$. This can be thought of as a duality equivalent of the obvious fact that the resonance region in M^2 does not scale in x. The stationary target here permits sufficient mass resolution to explore in detail the x dependence near $x = 1$ in a manner that is difficult at the ISR.

4.- NEUTRINO AND MUON EXPERIMENTS.- As indicated in figures 3 and 4 and in more detail in figure 7, the neutrino area is a complex one, with capability for neutrino, muon and hadron beams. The characteristics of the various beams are given in Table 3. This table is slightly futuristic in that the neutrino horn beam (NO-2) is just now being installed and the N5 beam does not quite exist, but otherwise is a fairly honest statement.

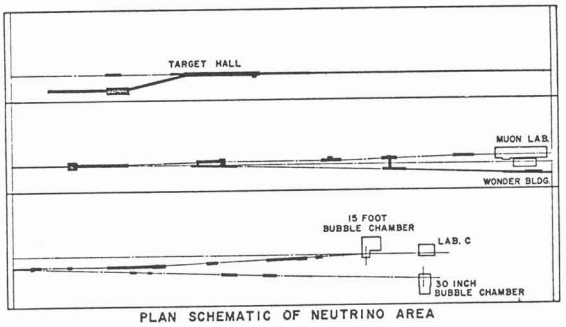

FIG. 7.- Plan of the neutrino area. The 2 km line is broken into three segments. The target hall where pions and K-mesons are produced and the subsequent decay region is shown at the top. The branching of the muon and hadron beams is shown next, along with the muon laboratory and one of the neutrino experiments (Wonder Building). The last segment indicates the location of the two bubble chambers and another neutrino experiment (Lab C).

TABLE 3

Neutrino Area Beams

1 July 1973

Beam	Production Angle mrad	Maximum Momentum GeV/c	Solid Angle μ sr	Momentum Acceptance Δp/p	Approx. Flux per 10^{13} Interacting Protons at 300 GeV
NO-1 Quadrupole Narrow Band Neutrino Beam	0	300	4-16	± 5%	10^6 neutrinos through $1m^2$
NO-2 Broad Band Horn Focus Neutrino Beam	0	500	2800	5-500 GeV	10^{10} neutrinos through 15' BC Spectrum Peaks at 20 GeV
N1 Muon Beam	0	300		± 2%	10^6 μ^+ at 150 GeV/c
N3 Hadron Beam for 30" BC	Variable $0 \leq p_T \leq 1$GeV/c	500	0.3	±.07% → ±1.2%	Sufficient for Bubble Chamber
N5 Hadron beam for 15' BC	Variable $0 \leq p_T \leq 1$GeV/c	500	0.3	±.02% → ±0.6%	Sufficient for Bubble Chamber

4.1.- NEUTRINO BEAMS AND EXPERIMENTS.- The neutrino experimental program in addition to the 15 foot bubble chamber presently consists of two approved experiments, both of which have had some considerable running and a few publications. These are the Harvard-Pennsylvania-Wisconsin-NAL experiment (NAL # 1A) located in Lab C of figure 7 and tha Cal-Tech-NAL experiment (NAL # 21) in the Wonder Building. The apparatus and most interesting early results of these experiments are described in some detail in Musset's report in these proceedings [4]. Thus there is no need for discussion here. It is, however, useful to mention briefly the two types of neutrino beams available at NAL.

The first type is the so-called broad band beam

that is utilized by experiment 1A. The running to date has been with a bare target and an event rate of the order of 15/hour with 300 or 400 GeV protons incident on the target. The broad band horn, presently being installed and to be tested in September, will increase the event rate considerably. The calculated energy spectrum of the neutrinos is shown in figure 8 for two incident energies. It is expected that the event rate in experiment 1A with this beam will be

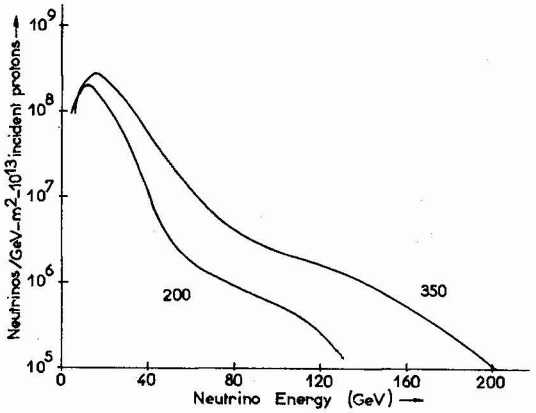

FIG. 8.- Calculated energy spectrum of neutrinos from the broad band horn beam (NO-2 of Table 3) for 200 and 350 GeV protons incident.

Proton Energy	350 GeV	200 GeV
Total ν Flux $\nu/m^2 - 10^{13}$ inc. p	6.8×10^9	3.8×10^9
Events/Pulse (20 m³ H_2, $\sigma_+ = 0.8\ E_\nu\ \sigma_0$)	0.1	0.04
Events/hour	45 (8 sec)	36 (4 sec)

Beam Geometry - as constructed; Focusing System - 2 horns as designed; Hagedorn Ranft Model; Thick Target- 40 cm long, 1 Interaction Length, Flux averaged over 2.7 m ϕ.

~ 150/hour for E_ν ~ 40 GeV and ~ 30/hour for E_ν >50 GeV.

The second neutrino beam is the so-called dichromatic or narrow band beam (NO-1 of Table 3). This beam is utilized by experiment 21. Its calculated neutrino energy spectrum is shown in figure 9 for 300 GeV protons incident and the beam tuned for 150 GeV. This beam is presently in operation and was used considerably in August. The average energy of the neutrinos from π decay is ~ 50 GeV, and from K decay is ~ 130 GeV. The event rate in experiment 21 is typically ~ 10/hour.

4.2.- MUON EXPERIMENTS.- In the neutrino area there is a high-energy muon beam (N1 of Table 3) into the muon laboratory, as shown in figure 7. This beam is

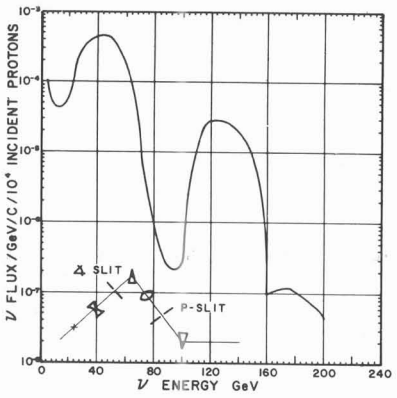

FIG. 9.- Calculated energy spectrum of neutrinos for the dichromatic or narrow band beam (NO-1 of Table 3) for 300 GeV protons incident and the beam tuned to 150 GeV. Target length .3 m; interaction MFP .293 m; front radius .002 m; collimator apertures: angle slit .25 in, momentum slit 2.50 in; decay pipe: length 397.6 m, radius .5 m; shield 1000.0 m; detector radius .5m; ν_e background not included.

not the ultimate in intensity or other properties, but now seems adequate for some interesting experiments. With a recently improved target load the beam has a μ/p ratio of ~ 2×10^{-8} at 150 GeV, corresponding to 10^5 muons per 5×10^{12} protons. The momentum resolution is $\Delta p/p \simeq 0.04$ and the halo is ~ 30%. There is another factor of 2 or 3 available soon, but orders of magnitude improvement in the intensity or halo would involve a large effort.

The presently approved program for muon physics consists of two experiments. The first is a Cornell-Michigan State-Princeton collaboration (NAL experiment #26) and is a test of Bjorken scaling in deep inelastic muon scattering. Figure 10 shows the apparatus

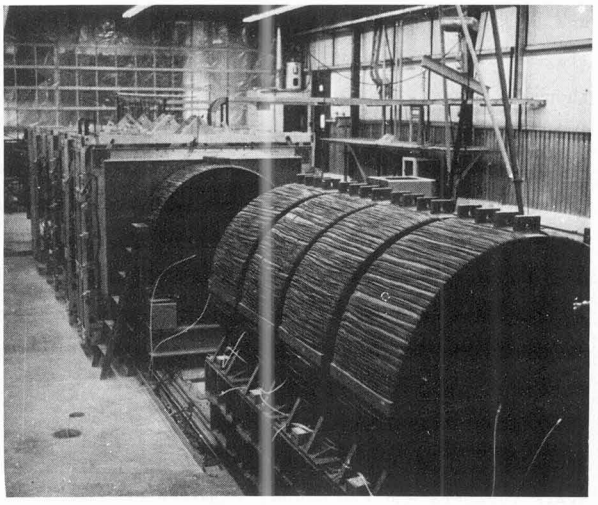

FIG. 10.- Apparatus for test of scaling in deep inelastic muon scattering (NAL experiment #26).

at an early stage of installation. The beam comes towards the viewer. At the rear, nearest the viewer, are the toroidal bending magnets for measurement of the muon momentum. In front are spark chambers and further forward out of sight is the heavy element target block. The whole apparatus is on rails and can be adjusted in the longitudinal dimension for different energies so that if scaling holds the distribution of events in the apparatus will be the same. The Q^2-ν region covered by this experiment is shown in figure 11, as is the region spanned by the electron experiments at SLAC. This experiment

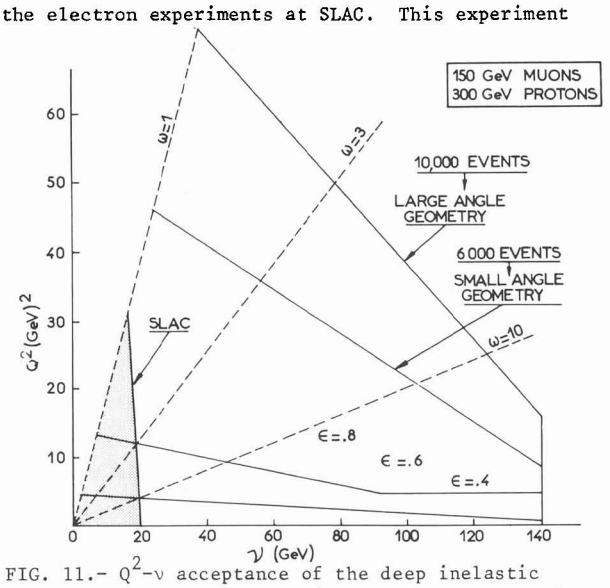

FIG. 11.- Q^2-ν acceptance of the deep inelastic muon scattering experiment # 26.- The shaded region indicates the domain covered by the electron experiments at SLAC.

already has data with 150 GeV incident muons (16 K events with $Q^2 > 2$ $(GeV/c)^2$, 1 K of them with $Q^2 > 20$ and 10 K of them with $\nu >$ 20 GeV) in the analysis stage and is running at 60 GeV to obtain a few thousand events. In October, 1973 it will run with 100 GeV muons and accumulate 10-15 K events. A second phase with the muon beam upgraded to 10^6 μ/pulse is anticipated six to nine months from now. Certainly there will be an enormous extension of the known Q^2-ν domain when these data are analyzed.

The second muon experiment is # 98, a Chicago-Harvard -Oxford collaboration. This is a study of inelastic muon scattering with a large spectrometer to analyze the hadronic final state as well as the muon. The spectrometer employs proportional wire and wire spark chambers and the magnet from the Chicago synchrocyclotron (the one used by Fermi and collaborators in the discovery of the 3,3 resonance almost 20 years ago). It also has the steel from the Rochester cyclotron as a muon selector in front of the target. The target is a heavy element at present, but eventuall will be hydrogen. The large program with this apparatus anticipates study of the deep inelastic structure functions, hadronic multiplicities, specific inelastic channels, as well as the $Q^2 \to 0$ limit of photoproductio The Q^2-ν range is roughly one half of that shown in figure 11. This experiment has been tested and is momentarily beginning to take real data.

5.- EXPERIMENTS IN THE INTERNAL TARGET AREA.- The internal target area is located approximately one third of the way around the main ring at an access building designated C-O, as shown in figure 3. The area is just a normal part of the main ring tunnel, apart from the targets and straight section.. Quarters are therefore rather cramped and apparatus must be constrained in size, at least laterally. In spite of space limitations, at least 4 separate experiments have operated simultaneously in this area. Its great virtue and reason for its popularity is the availability of incident protons of any energy from the injection energy of 8 GeV to the maximum energy of the machine. Until recently there was one target station with two targets, a removeable rotating target of polyethylene foils and carbon filaments and the pulsed gas jet target built in the U.S.S.R. There is now a second rotating foil target upstream about 100 feet from the first.

The gas jet target assembly and some elastic scattering apparatus are shown in place in figure 12. The

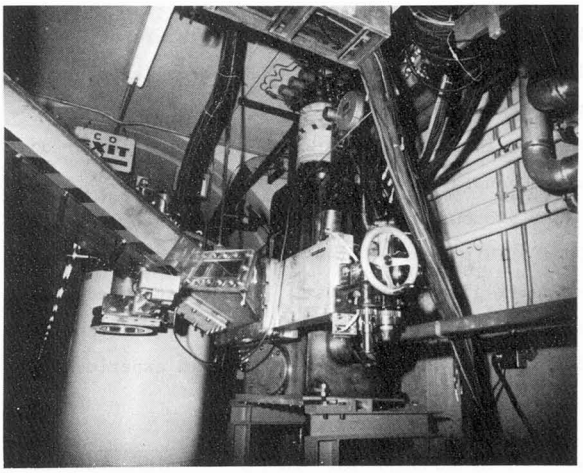

FIG. 12.- U.S.S.R. pulsed gas jet target assembly and apparatus of the joint U.S.-U.S.S.R. elastic scattering experiment in the internal target area.

accelerator beam pipe runs off to the right. The hydrogen source and associated cryogenics are located in the centre above the light rectangular box. The recoil arm of the elastic scattering apparatus extends diagonally upwards to the left. The pulse of hydrogen "gas" (sometimes droplets, sometimes snow) is projected downwards across the accelerating beam at any chosen time during the acceleration ramp thereby selecting the energy of interaction. Several pulses per ramp are possible in principle but are rarely used.

The presently approved program at the first target of C-O consists of

1) p-p elastic scattering at small $|t|$
2) p-p and p-d inelastic proton spectra
3) single photons at small $p_\perp$
4) single photons at large $p_\perp$ and $\theta_{cms} \simeq 90^\circ$
5) p-d elastic scattering at small $|t|$
6) pp Jacobian peak missing mass search

At the newly created upstream target there are two experiments being installed:

1) Inelastic pp recoil proton spectra at small $|t|$
2) Search for heavy leptons.

Of the six experiments at the gas jet target station, the first three have completed their runs and are in various stages of analysis and publication. The fourth is essentially complete and the fifth and sixth are just nicely begun.

5.1.- U.S.-U.S.S.R. ELASTIC AND SLIGHTLY INELASTIC p-p SCATTERING EXPERIMENT.- As a first sample of results from the gas jet target there are the data from the U.S.-U.S.S.R. collaboration on the slope of the elastic p-p scattering cross section at small $|t|$. These results [5] are shown in figure 13 along

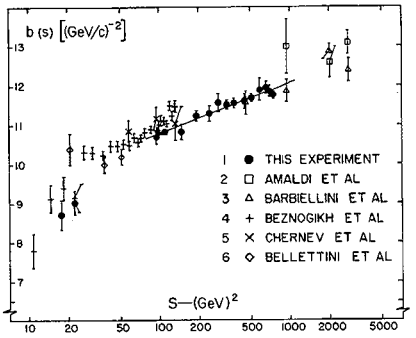

FIG. 13.- Slope parameter $b(s) = \frac{d}{dt} \left| \ln \frac{d\sigma}{dt} \right|$ for p-p elastic scattering at $0.005 < |t| < 0.09$ (GeV/c^2) as a function of s. The solid dots are the results of the NAL gas jet experiment. Figure from ref. 5.

with earlier data from Serpukhov and elsewhere at lower energies and the ISR at higher energies. The data show continued shrinkage of the forward diffraction peak up to 400 GeV.

From analysis of the very small $|t|$ region including the beginnings of the Coulomb peak the U.S.-U.S.S.R. collaboration will shortly have results on the ratio of the real to imaginary part of the forward scattering amplitude. This is of great interest because of the increase in the total cross section reported at ISR energies. Analyticity arguments show that any significant rise in the total cross section must be accompanied by a change in sign from negative to positive of the ratio of real to imaginary part. The cross-over is expected roughly at the point where the rise in total cross section begins [6].

Along with the elastic data are recorded the inelastic scattering events for modest missing mass. Preliminary results [7] show that for the inelastic reaction $pp \to pN^*(1400)$ at 200 GeV the differential cross section is approximately the same in magnitude and shape as at 15-20 GeV. It thus appears that the $N^*(1400)$ production is a truly diffractive and roughly energy-independent process like elastic scattering.

5.2.- INCLUSIVE PROTON SPECTRA IN $pp \to pX$.- A Rutgers -Imperial College collaboration has completed an experiment on inelastic proton-proton scattering at energies from 50 to 400 GeV. Some results have already been published and others submitted to this conference [8,9]. The experiment covers a $|t|$ range of $0.15 < |t| < 0.4$ $(GeV/c)^2$ and an x interval of $0.80 < x < 0.94$. Within this domain the data on the inclusive invariant cross section are consistent with a paremetrization of the form,

$$s\frac{d^2\sigma}{dtdM^2} = A(x)e^{b(x)t}\left[1 + \frac{B(x)}{\sqrt{s}}\right].$$

The slope parameter is found to be $b \simeq 6$, independent of x, while the non-scaling fraction of the cross section (the $B(x)/\sqrt{s}$ term) is larger at larger x values. This behaviour is illustrated in figure 14 where data are displayed for a series of four t values and two x values. The open circles ($x = 0.91$) consistently show a steeper slope in $s^{-\frac{1}{2}}$ than the solid points ($x = 0.83$). These data show very prettily the approach to scaling and agree with the conclusions mentioned in Section 3.4.3 from the bubble

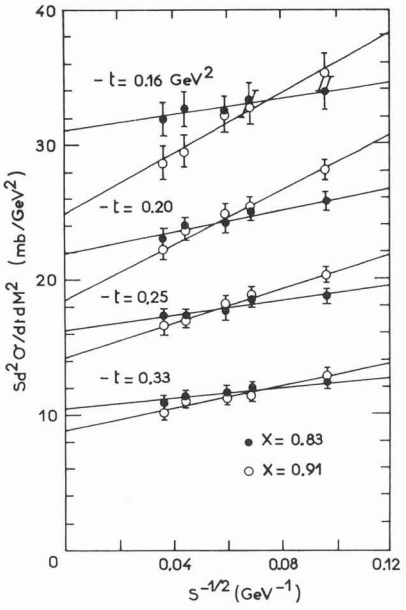

FIG. 14.- The behaviour of the invariant cross section for pp → pX as a function of $s^{-\frac{1}{2}}$ at a set of four t values and two different x values. Figure from ref. 9.

chamber that the non-scaling contributions are more important closer to x = 1. The authors have attempted several triple Regge fits to their data; the fits are not conclusive, however, data at x > 0.94 being required to remove ambiguities.

The Rutgers-Imperial College group had some running with the gas jet providing a deuterium target instead of hydrogen. Analysis of the recoil proton data permits extraction of the cross section for pn → pX, smeared by the Fermi motion inside the deuteron. Such data are of considerable interest theoretically because they provide information on triple Regge couplings in which two of the Reggeons have I = 1. The scaling terms would then be A_2A_2P, $\rho\rho P$, $\pi\pi P$, etc. The x-dependence of the invariant cross section differs for the different Reggeons. Near t = 0, for example, the A_2A_2P or $\rho\rho P$ contributions ($\alpha_R \simeq \frac{1}{2}$) give a constant cross section as x → 1, while the $\pi\pi P$ term ($\alpha_R \simeq 0$) vanishes linearly. Preliminary results show that at $|t| = 0.16\ (GeV/c)^2$ the cross section for pn → pX at x ≃ 0.82 is about 60% of the pp → pX and falls roughly linearly towards x = 1. Such a behaviour is consistent with an appreciable contribution from $\pi\pi P$, but does not exclude (and probably requires) other terms as well.

6.- PROTON LABORATORY.- The proton area shown in figure 3 is actually a series of underground laboratories more or less tailored to individual experiments. The present layout is shown in figure 15 and in an early stage of construction in figure 16. The upper

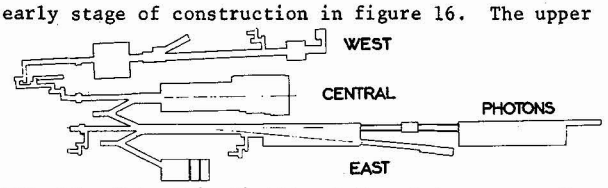

FIG. 15.- Schematic diagram of the proton area. The beams from the switchyard enter from the left after approximately 1 km of drift space without focussing magnets. From top to bottom the laboratories are called "West", "Central" and "East".

FIG. 16.- The proton area at an early stage of construction, looking towards the source of protons. The neutrino beam line berm is visible parallel to the road on the right.

laboratory (on the right in figure 16) is in line of sight of the source of beam in the switchyard. At present this lab. is not in operation for experiments. It may be necessary to install quadrupoles upstream in order to reduce the proton halo to acceptable limits. In proton east and proton central the spot size is quite good even after the 1 km of free flight.

6.1.- APPROVED PROGRAM.- The presently approved program in the proton area covers a diversity of physics goals. The experiments are:

1) Lepton search, looking at the production of single electrons initially, and later of electron and muon pairs, in single, then double-arm spectrometers. Heavy

objects decaying into leptons are the object of the search.

2) Particle (hadrons and leptons) search at large $p_\perp$, with a long single arm spectrometer (see below).

3) Photoproduction search, looking for diffractive production of hadronic states and photoproduction of W bosons, heavy leptons, etc. in an untagged photon beam.

4) Total photon cross section measurements with a tagged photon beam up to 300 GeV.

5) Particle production, with a double focussing spectrometer looking at backwards particles in the lab. and covering $-1 < x < -0.1$, $0 < p_\perp < 2$ GeV/c.

6) Single and double photon search at large angles, studying π^o production via the single gammas and searching for heavy neutral objects decaying into two photons.

7) Muon search, looking for heavy particles decaying into muons.

8) Magnetic monopole search.

9) Proton-proton elastic scattering at large angles ($\sim 3 < |t| < 15$ (GeV/c)^2).

In the present time frame the first two experiments are taking data, the first in proton central and the second in proton east. The third experiment is almost installed and ready to run. It is located in the extension to proton east shown in figure 15. Its target is in the same location as that for the second experiment, but only one can have beam at a time. These three experiments will be running during the coming year and even beyond. The particle search (#2) already has interesting results to be described briefly below.

Experiments 6, 7 and 9 are intended for the proton west area and are 6 months to a year away with still some questions about improvements of the beam.

6.2.- TAGGED PHOTON BEAM.- Experiment 4 (and a number of proposed but not yet approved experiments) needs a tagged photon beam. There is still discussion about the development of this beam, but it will be located in the area behind proton east and will probably be built in two phases. The first phase is a two-stage electron and tagged photon beam with energies up to 300 GeV. Illustrative intensities with 500 GeV protons incident at 10^{13} protons/pulse are 1.5×10^8 electrons at 150 GeV and 4×10^7 electrons at 300 GeV, with $\Delta p/p = \pm 2\%$. This phase should be in operation within 12-18 months. The second phase is to be a 4-stage beam, but its properties must await study of such things as the π/e ratio in the first phase. Ultimately an electron, tagged photon and pion beam of high energy and good intensity will exist in the proton area.

6.3.- PRODUCTION OF CHARGED HADRONS AT LARGE TRANSVERSE MOMENTA.- Preliminary but very interesting results are now available from a Chicago-Princeton collaboration (NAL experiment #100) on the production of charged hadrons at large $p_\perp$ and roughly 90^o in the c.m.s. These data were presented at this conference by Cronin [10]. A schematic diagram of the apparatus is shown in Figure 17. Most of the data have been taken with 300 GeV and now 200 GeV protons on a tungsten target. The energy is smeared by Fermi motion of the nucleons in the target by approximately ± 4 GeV around that for a proton on a stationary nucleon. The Cherenkov counters permit clean separation of pions, K-mesons and protons or antiprotons over the range $0.7 < p_\perp < 7$ or 8 GeV/c at c.m.s. angles within $\pm 20^o$ of 90^o.

A sample of these data is given in figure 18 where the invariant inclusive differential cross section for $pW \to \pi^-$ + anything versus $p_\perp$ is displayed. For $p_\perp < 2$-3 GeV/c the data agree very well in shape with the Saclay-Strasbourg results from the ISR at equivalent energies. But at larger $p_\perp$ the spectra fall more steeply with increasing $p_\perp$ than the $pp \to \gamma X$ data at higher ISR energies. From parton models of various sorts it is expected that the invariant cross section should be of the form, $Ed^3\sigma/d^3p \simeq s^{-n}F(x_\perp)$, where $x_\perp = 2p_\perp/\sqrt{s}$ is the transverse analogue of Feyman's x variable. For $p_\perp \gtrsim 3$ GeV/c the data of figure 18 are consistent with this form, with $n \simeq 5^+$. Parton models with gluon exchange tend to have n = 2 while some other models have n = 4. Theorists will obviously work on this problem! On the experimental side, data will be taken at 400 GeV in order to tie down the energy dependence more precisely and to overlap significantly with the ISR energies.

The results on charged particle ratios as functions of $p_\perp$ at 300 GeV are shown in figure 19. The data at 200 GeV are similar. The ISR results at $0 < p_\perp < 3$ GeV/c indicate a rise in all of these ratios. The turnovers at larger $p_\perp$ in figure 19 are

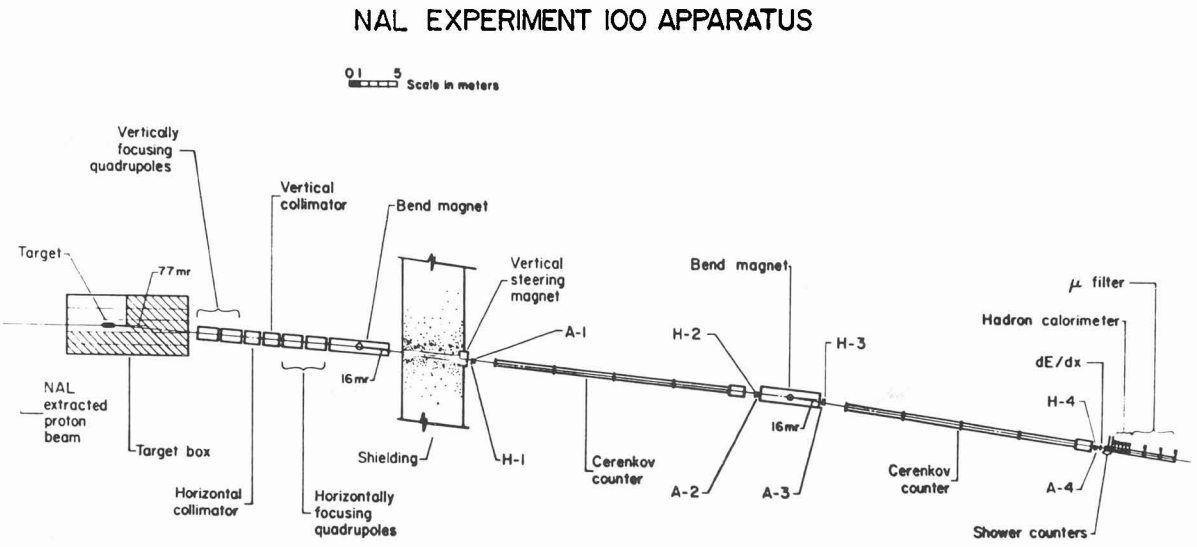

FIG.17.- Schematic diagram of NAL experiment # 100 ((2) of list of approved experiments). The overall length is 110 meters, with two momentum measurements and two long Cherenkov counters, plus associated detectors for hadrons and leptons.

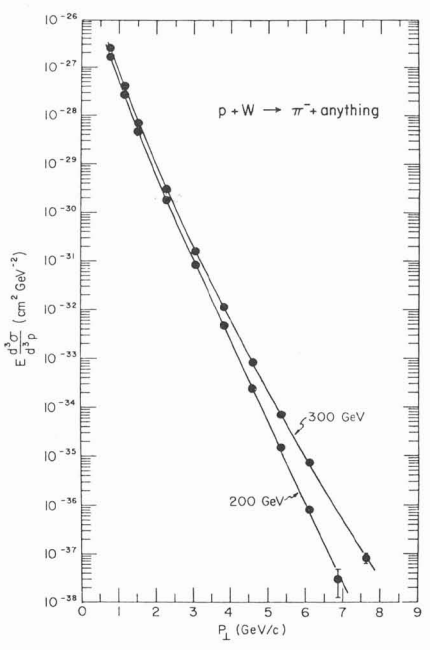

FIG. 18.- Invariant differential cross section for $pW \to \pi^- X$ at 200 and 300 GeV versus $p_\perp$ at angles near 90° in the c.m.s. Figure is from reference 10.

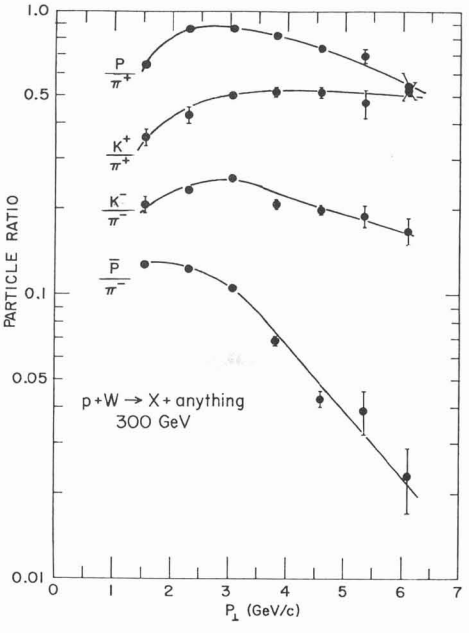

FIG. 19.- Particle ratios versus $p_\perp$ at roughly 90° in c.m.s. for pW interactions at 300 GeV. Figure is from reference 10.

quite dramatic. Quark-parton models generally assume that the high momentum components inside a hadron are carried by the valence quarks. Such models [11] therefore predict a rapid decrease in $\bar{K}/\pi$ and $\bar{p}/\pi$ ratios at large $p_\perp$ because all the quarks necessary for the formation of $\bar{K}$ or $\bar{p}$ in p-p interactions must

come from the "sea". On the other hand, the K^+/π^+ ratio should eventually become independent of $p_\perp$. These expectations seem to be borne out by the data of figure 19. One possible problem for theorists is the relatively large value of the p/π^+ ratio over a wide range of $p_\perp$.

7.- MESON LABORATORY.- On the opposite side of the neutrino beam line is the meson area, as shown in figure 3. This area is the last one to be commissioned, although its first experiments (emulsion exposures) were done one year ago. A detailed schematic is shown in figure 20 and a photograph of the meson laboratory from the air in figure 21. The hall itself is relatively short (~ 100 m). Experimental targets are therefore sometimes located upstream of the hall (see figure 20) and detection apparatus in long appendages downstream. Support for this equipment is provided by long concrete pads and shelter by corrugated iron wonder buildings.

As indicated in figure 20 there are six beams in the meson laboratory. The general properties of these beams are described in Table 4. At present and for some time in the future the so-called "test" beam (M5) does not exist. The beams are spread across the hall at ground level, except for the K^o beam (M4) which is located below the neutron beam (M3). The roof of the M4 tunnel is visible in figure 21 at the centre line of the meson laboratory.

7.1.- APPROVED MESON LABORATORY PROGRAM.- The five existing beams in the meson laboratory have associated an extensive approved program that is

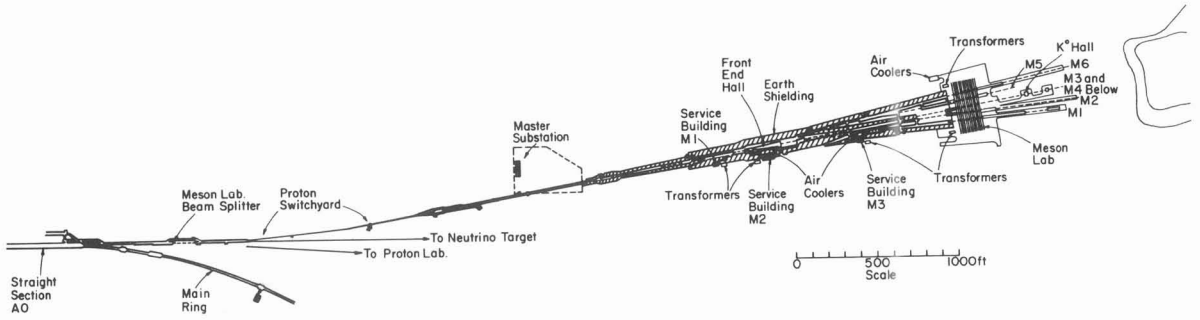

FIG. 20.- Schematic of the meson area from the switchyard to the meson laboratory itself. From the beam splitter to the front of the meson lab is approximately 1.5 km.

FIG. 21.- Aerial view of the meson laboratory. The beams enter the hall from the bottom right, having been produced in underground target stations 300-400 metres upstream. Pads and one wonder building appendage can be seen on the far side of the hall.

TABLE 4

Meson Area Beams

1 July, 1973

Beam	Production Angle mrad	Maximum Momentum GeV/c	Solid Angle μsr	Momentum Acceptance Δp/p	Approx. Flux per 10^{13} Interacting protons at 300 GeV
M1 High Energy	3.91	200	2.0	±0.1%→±2.0%	10^7 π at 150 GeV
M2 Diffracted Proton Beam	1.75	300	0.22	±0.1%→±1.4%	10^{10} p at 200 GeV
M3 Neutron Beam	1.75		Variable		$10^8/cm^2$
M4 K^o Beam	6.5		Variable		$10^6/cm^2$
M5 Medium Energy	20.0	50	6.2	±0.05%→±0.5%	10^6 π at 50 GeV
M6 High Energy High Resolution	3.05	200	1.34	±0.014%→±1.0%	10^7 π at 100 GeV

just beginning. It is estimated that it will take 2 to 3 years to run off this program and closely related follow-on experiments. Only the briefest listing of these experiments is possible in this report. The sorting is according to beams and in approximate order of running.

7.1.1.- M1 beam.- This beam is a high-energy, moderate resolution hadron beam with charged hadrons up to 200 GeV. The approved experiments are

1) Total cross section measurements from 20 to 200 GeV with $\pi^{\pm}$, $K^{\pm}$, $p^{\pm}$ on H_2 and D_2 targets, with 0.1% relative accuracy as a function of energy as a goal. This experiment is beginning to run and will produce results in the next 9 months.

2) $\pi^{\pm}p$ and p-p differential elastic scattering at 50 - 170 GeV/c and $0.1 < |t| < 2\text{-}3\ (\text{GeV/c})^2$ with a double arm spectrometer. This experiment is now being installed and will be in full operation by mid-1974.

3) $\pi^{\pm}$, $K^{\pm}$ -p inclusive distributions.

4) Elastic scattering with a polarized target.

5) Diffractive production of mesonic systems from helium using a streamer chamber.

7.1.2.- M2 beam.- This beam is a diffracted proton beam that also has meson capability. The approved experiments in this beam are

1) Quark search - this experiment has now completed its running. Preliminary results are described below.

2) Pion-nucleon charge exchange differential cross section at energies from 20 to 200 GeV and $0 < |t| < 1.5\ (\text{GeV/c})^2$. The process $\pi^- p \to \eta n$ will also be studied. This experiment is in place and has by now begun to take data.

3) Inclusive distributions from π, K, p interactions in H_2 in the projectile fragmentation region ($M^2 < 15\ \text{GeV}^2$) and $0.2 < |t| < 0.4\ (\text{GeV/c})^2$. This missing mass spectrometer experiment is to look for new heavy bosons as well as inclusive spectra.

4) Neutral hyperon production and interaction. This experiment involves the creation of a neutral hyperon beam and its use to study hyperon total and possibly differential cross sections at energies of 100-200 GeV. It will follow the second experiment above.

5) Charged hyperon beam.

7.1.3.- M3 beam.- This beam is a neutron beam with energies up to 300 GeV. The approved experiments are

1) Neutron-proton total cross sections from 40 to 300 GeV. The accuracy expected is ±2% on the cross sections, with the neutron energy determination in a total absorption spectrometer to 10% FWHM. This experiment is in place and running.

2) n-p elastic diffractive scattering. This experiment is by the same group as (1) and will follow it.

3) n-p charge exchange (backward n-p elastic) scattering.

4) Neutron dissociation for 50 to 200 GeV neutrons incident on heavy elements. This experiment is to look at "Vee" events ($n \to p\pi^-$) in a magnetic spectrometer arising from the dissociation of the neutron via electromagnetic and hadronic interactions.

7.1.4.- M4 beam.- This is a neutral K-meson beam for regeneration and other experiments. Approved are

1) Quark search. This experiment by a BNL-Yale collaboration has been completed.

2) K^0 regeneration at high energies. The aim is to study all aspects of regeneration as a function of energy, to test the Pomeranchuk theorem, etc. Some equipment is in place. Running is expected in early 1974.

7.1.5.- M6 beam.- The M6 beam is a high-energy, high-resolution beam. Its presently approved experiments are:

1) Elastic scattering of hadrons at energies up to 200 GeV and $|t| < 0.2\ (\text{GeV/c})^2$. This single-arm set-up uses two magnets and high pressure magnetostrictive chambers with high resolution. It will explore very small $|t|$ values, into the Coulomb interference region.

2) Elastic and inelastic scattering of hadrons by hydrogen and deuterium from 50 to 200 GeV and $0 < |t| < 1.5\ (\text{GeV/c})^2$. The apparatus consists of a focussing spectrometer located in the long and slightly curving Wonder building in figure 21. The magnets and counters are now in place and being tested. Data taking should begin in early 1974.

3) Multiparticle production of hadrons. This experiment consists of a large (the people's) spectrometer to be located next to experiment (2), on the concrete pad furthest to the left in figure 21. It is a multipurpose device that will presumably be in place for several years. A switch in the M6 beam will feed beam to this experiment or to (2).

4) Projectile fragmentation studies.

5) Backward $\pi^{\pm}p$ elastic scattering.

6) Associated production at high energies.

The last three experiments are not approved in their entirety pending the performance of the second listed experiment and its results. They will employ much the same apparatus if and when they are done.

7.2.- QUARK SEARCH RESULTS.- The two quark search experiments have now been completed. No quarks have been positively identified. In the BNL-Yale experiment in the M4 beam line preliminary results indicate that for quark masses on the interval $3 < M_q < 12$ GeV the production cross section per nucleon is less than 10^{-35} cm^2 for 200-300 GeV protons incident.

The NAL experiment in the M2 beam has just finished running during this conference. Two separate configurations of beam energy and bending magnet setting were used. One, favouring quarks of charge 2/3, had 300 GeV protons on Be and W targets and the bending magnets set at 207 GeV. This would yield quarks of 140 GeV in the lab., corresponding to quarks roughly at rest in the c.m.s., as would occur in pair production with masses up to 11 GeV. The second run was with 200 GeV protons on Be and the beam bending magnets set for 270 GeV. This favours quarks of charge 1/3 moving slowly in the c.m.s. ($M_q \leq 9$ GeV). In the first run, ~ 2×10^{16} protons, and in the second, 10^{17} protons, were incident on the target. With the last run (called "super momentum", with 200 GeV incident and 270 GeV in the bending line) backgrounds were extremely low. No certain quarks were found. The c.m.s. cross section $d^2\sigma/dp^* d\Omega^*$ limit varies from ~ 10^{-36} cm^2/GeV x steradian at the maximum mass (8.7 GeV for charge 1/3, 10.9 GeV for charge 2/3).

These negative results are not as exciting as finding quarks, of course. But as the experimenters push the limits lower and extend the range of mass values explored theorists must work harder. The answer may be in integrally charged quarks of the Han-Nambu variety, or in other directions.

Soon the meson lab will be producing positive as well as negative results. The rising p-p total cross section seen in cosmic rays and at the ISR makes the forthcoming NAL data on $\pi^\pm$, $K^\pm$, $p^\pm$ total cross sections especially significant.

8.- CONCLUSIONS.- The major results of the NAL experimental program so far are:

1) The several experiments on elastic scattering and inclusive proton and photon distributions from the gas jet target located at the internal target area. The variable energy aspect of this target is extremely important and useful.

2) The numerous experiments with protons and now positive and negative pions in the 30 inch hydrogen bubble chamber. Here the wider spaced energies still provide valuable information on the energy variation of the main features of multiparticle hadronic interactions.

3) The two neutrino experiments whose results on neutral currents, tests of scaling, limits on W-bosons and heavy leptons, etc. are described in Musset's report in these proceedings.

In the coming months (6 months - 1 year) there will be results on at least

4) Deep inelastic muon scattering.

5) Leptonic and hadronic phenomena at large transverse momenta.

6) Total cross sections up to 200 GeV for $\pi^\pm$, $K^\pm$, $p^\pm$ on hydrogen (and deuterium).

7) Differential elastic scattering at very small $|t|$ and for $0.1 < |t| < 2$ (GeV/c)^2 for mesons and nucleons on protons up to 200 GeV.

8) Photoproduction of diffractively produced hadron states (ρ, ρ's, ...) and also searches for new charged objects with masses up to 10 GeV.

The program described in this report is mainly a first generation of experiments. It will take 2 or 3 years to complete if one allows the possibility of some second generation experiments following immediately after the first. By the time the proceedings appear a number of anachronisms will exist in the text, but the overall view is reasonably correct.

As with most things the natives are ahead of us and successfully into the second generation of experiments, as figure 22 shows.

9.- ACKNOWLEDGEMENTS.- A report of this kind owes much to others. I wish to acknowledge the valuable assistance of J.R. Sanford and his staff, and R. Lundy, R. Orr, J. Peoples, R. Stefanski and A. Frelo in providing the most recent facts, tables and photographs about the laboratory. They are not responsible, however, for errors in my written report. My thanks go to all of the many experimenters who responded to

FIG. 22.- The native population at NAL is already into the second generation of experiments.

my request for information and results from their NAL experiments. My apologies go to the sub-set whose experiments received no or little mention. Fortunately they have recourse to the open literature.

References

[1] ALBROW (M.G.) et al., paper no. 375.
[2] BARISH (S.J.), COLLEY (D.C.), SCHULTZ (P.F.) and WHITMORE (J.), ANL/HEP 7338 (August, 1972).
[3] FERBEL (T.), private communication
FOA (L.), these proceedings.
[4] MUSSET (P.), these proceedings.
[5] BARTENEV (V.) et al. (USSR-USA collaboration), 73/54-EXP (August 1973).
[6] See, for example, the elementary discussion in JACKSON (J.D.), Proceddings of the 1973 Scottish Universities Summer School in Physics (to be published).
[7] GOULIANOS (K.), private communication.
[8] ABE (K.), et al., paper no. 190.
[9] ABE (K.), et al., paper no. 191.
[10] CRONIN (J.), oral presentation, this conference.
[11] See, for example,
ELLIS (S.D.) and KISLINGER (M.B.), NAL-PUB-73/40-THY (June 1973), submitted to this conference (paper no. 124).